

2015

Pirt contributes to uterine contraction - induced pain in mice

Qin Liu

Washington University School of Medicine

et al

Follow this and additional works at: http://digitalcommons.wustl.edu/open_access_pubs

Recommended Citation

Liu, Qin and et al, "Pirt contributes to uterine contraction - induced pain in mice." *Molecular Pain*.11, 57. (2015).
http://digitalcommons.wustl.edu/open_access_pubs/4663


This Open Access Publication is brought to you for free and open access by Digital Commons@Becker. It has been accepted for inclusion in Open Access Publications by an authorized administrator of Digital Commons@Becker. For more information, please contact engeszer@wustl.edu.

RESEARCH

Open Access



Pirt contributes to uterine contraction-induced pain in mice

Changming Wang¹, Zhongli Wang¹, Yan Yang¹, Chan Zhu¹, Guanyi Wu¹, Guang Yu¹, Tunyu Jian¹, Niuniu Yang¹, Hao Shi¹, Min Tang¹, Qian He¹, Lei Lan², Qin Liu³, Yun Guan⁴, Xinzhong Dong⁵, Jinao Duan^{1*} and Zongxiang Tang^{1*} 

Abstract

Uterine contraction-induced pain (UCP) represents a common and severe form of visceral pain. Nerve fibers that innervate uterine tissue express the transient receptor potential vanilloid channel 1 (TRPV1), which has been shown to be involved in the perception of UCP. The phosphoinositide-interacting regulator of TRP (Pirt) may act as a regulatory subunit of TRPV1. The intraperitoneal injection of oxytocin into female mice after a 6-day priming treatment with estradiol benzoate induces writhing responses, which reflect the presence of UCP. Here, we first compared writhing response between *Pirt*^{+/+} and *Pirt*^{-/-} mice. Second, we examined the innervation of Pirt-expressing nerves in the uterus of *Pirt*^{-/-} mice by immunofluorescence and two-photon microscopy. Third, we identified the soma of dorsal root ganglion (DRG) neurons that innervate the uterus using retrograde tracing and further characterized the neurochemical properties of these DRG neurons. Finally, we compared the calcium response of capsaicin between DRG neurons from *Pirt*^{+/+} and *Pirt*^{-/-} mice. We found that the writhing responses were less intensive in *Pirt*^{-/-} mice than in *Pirt*^{+/+} mice. We also observed Pirt-expressing nerve fibers in the myometrium of the uterus, and that retrograde-labeled cells were small-diameter, unmyelinated, and Pirt-positive DRG neurons. Additionally, we found that the number of capsaicin-responding neurons and the magnitude of evoked calcium response were markedly reduced in DRG neurons from *Pirt*^{-/-} mice. Taken together, we speculate that Pirt plays an important role in mice uterine contraction-induced pain.

Keywords: Pirt, Uterine contraction-induced pain, Dorsal root ganglion, TRPV1

Background

Study of uterine contraction-induced pain (UCP) that occurs during labor or menstruation (dysmenorrhea) has received little attention compared with the study of other visceral pain conditions. The uterus is innervated by afferent hypogastric nerve fibers through which any sensory information is transmitted to the central nervous system (CNS) [1]. Although the hypogastric nerve also transmits noxious mechanical and chemical stimuli, pain induced by uterus cervical distension shows similarity to the heat hyperalgesia observed in animal models [2]. This similarity suggests a potential role of heat-sensing

ion channels in pain induced by cervical and uterine contraction. Indeed, the transient receptor potential vanilloid 1 (TRPV1), which is important to the detection of noxious heat, may contribute to the perception of visceral pain [3–6].

Previous studies have also suggested an important role of estrogen in the modulation of visceral pain. Sex hormones may underlie gender differences in pain perception and in analgesia [7]. Estrogen was suggested to contribute to visceral pain hypersensitivity and to the increased sensitivity to visceral pain in animal models [2, 8–10]. Moreover, estrogen may amplify pain responses to uterine cervical distension in animal models by enhancing TRPV1 function [11]. Estrogen not only increased TRPV1 expression in afferent sensory neurons innervating the uterus [10], but also exaggerated the uterine pain

*Correspondence: dja@njutcm.edu.cn; zongxiangtang@njutcm.edu.cn

¹ College of Basic Medicine, Nanjing University of Chinese Medicine, 138 Xianlin Rd, Nanjing 210023, Jiangsu, China

Full list of author information is available at the end of the article

evoked by capsaicin and heat stimulation [11]. On the other hand, the activation of nerve fibers in the uterine horn was reversed by intrauterine pretreatment with capsaizine, a TRPV1-selective antagonist [11, 12]. The level of TRPV1 expression in ectopic endometrium is also correlated with the severity of dysmenorrhea in patients [13]. These findings suggest an important role of TRPV1 in uterine pain perception [12].

The phosphoinositide-interacting regulator of TRP (Pirt) is a transmembrane protein that is expressed in most nociceptive neurons in the dorsal root ganglia (DRG), but not in CNS. Pirt has recently been identified as a key component of the TRPV1 and TRPM8 complexes and acts as an endogenous enhancer of TRPV1 and TRPM8 function, [14, 15]. Since TRPV1 participated in UCP [10, 11, 14], we hypothesized that Pirt may also play an important role in the perception of UCP by interacting with TRPV1. In the present study, we demonstrated that Pirt was involved in the perception of UCP.

Methods

Animals

This study was approved by the Animal Care and Use Committee of Nanjing University of Chinese Medicine (Nanjing, China). Experiments were conducted according to the animal research ethical guidelines of the International Association for the Study of Pain. Female C57BL/6 mice were housed in groups of four per cage in our GLP animal center, with free access to food and water.

Pirt^{-/-} mice were bred in the laboratory of one of the authors (XD). For the generation of *Pirt*^{-/-} mice, the entire Pirt coding region was replaced with an EGFPf-IRESrtTA-ACN- targeting construct to produce a null allele [14]. Offspring *Pirt*^{-/-} and *Pirt*^{+/+} littermates were generated by breeding heterozygotes. Only healthy animals weighing 15–20 g and displaying normal water and food intake were included in the study.

Behavior analysis

Animal behavior experiments were performed in a controlled environment of 20–24 °C, 45–65 % humidity, and a 12-h day/night cycle. Female *Pirt*^{+/+} and *Pirt*^{-/-} mice (5–6 weeks old) were used in all experiments. Animals were acclimated to the testing environment for 30 min before the initiation of writhing behavior tests. Estradiol benzoate was administered by intraperitoneal (i.p.) injection daily at 9 a.m. for 6 consecutive days (0.01 g/kg/day). One day after estradiol priming (i.e., day 7), oxytocin was injected (0.01 L/kg, i.p.) to induce uterine contractions. Writhing behavior responses were recorded with a digital video camera (HDR-PG820E, Sony, Minato, Tokyo, Japan) for 80 min after oxytocin injection. Abdominal writhing was defined as an exaggerated extension of

the abdomen combined with the outstretching of the hindlimbs [16]. Animal behavior (e.g., the number of writhing motions) was analyzed by investigators who were blind to animal treatment conditions.

Real-time PCR

Total RNA was extracted from freshly isolated DRG using TRIzol reagent (Invitrogen) and treated with RQ1 Dnase (Promega). The reverse transcription was performed using the Transcript First Strand cDNA Synthesis kit (Roche, Basel, Switzerland).

For qPCR, Light Cycler 480 SYBR Green I Master (Roche, Basel, Switzerland) was used. The reaction was run in an Lihtg Cyler 480 II Real-Time PCR instrument (Roche, Basel, Switzerland) using 1 μL of the cDNA in a 20 μL reaction according to the manufacturer's instructions. The sequences of the mouse Pirt primers were as follows: forward primer: TAGACGAGAGGTCTC-CAGAGT; reverse primer: CCAGTTGCTTTTGGGT-GTGG. The sequence of mouse GAPDH primers were as follows: forward primer: ACCACAGTCCATGCCAT-CAC; reverse primer: TCCACCACCCTGTTGCTGTA. Calibrations and normalizations were done using the following $2^{-\Delta\Delta CT}$ method: where $\Delta\Delta C_T = (CT_{\text{target}} - CT_{\text{reference}}) - (CT_{\text{calibrator}} - CT_{\text{reference}})$. GAPDH was used as the reference gene for qPCR experiments.

Uterine tissue extraction and H&E-staining

For uterine tissue retrieval, mice were anesthetized with 1 % sodium pentobarbital (50 mg/kg, i.p.), and perfused transcardially with 10–15 mL phosphate-buffered saline (PBS) followed by 10–15 mL of ice-cold 4 % paraformaldehyde (pH 7.4). We performed a laparotomy via a lower abdomen midline incision to dissect and remove the uterus. Then we post-fixed the uterus in 4 % paraformaldehyde in PBS for 3 h and stored it overnight in 30 % sucrose for cryoprotection. The uterus was then embedded in optimum cutting temperature compound (OCT, Leica, Wetalar, Germany) and rapidly frozen at -20 °C (CM1950, Leica). Cryoembedded tissues were cut into 10-μm thick slices on a sliding microtome (CM1950, Leica). Conventional H&E-staining technique was used to confirm the distribution of Pirt nerve fiber terminals on the uterus. All imaging was performed with an Olympus fluorescence microscope (BX51, Olympus, Shinjuku, Tokyo, Japan).

Detecting Pirt-expressing nerve fibers in the uterus

We used fluorescence microscopy to examine Pirt-expressing nerve fibers in the uterus of *Pirt*^{-/-} mice. Because of the EGFPf-IRESrtTA-ACN-targeting construct in *Pirt*^{-/-} mice, Pirt-expressing neurons and nerve

fibers can be identified by green fluorescence, the expression of which is driven by the endogenous *Pirt*-promoter gene. Adjacent uterus sections were stained with hematoxylin and eosin (H&E), and overlapping fluorescence (*Pirt*) with bright-field (H&E) images allowed us to identify the histological site of *Pirt*-expressing nerve fibers in the uterus. Images were acquired and overlapped by using stereological software (Stereo Investigator 10, MBF, Williston, VT, USA).

Two-photon microscopy imaging

Uteruses from *Pirt*^{-/-} mice were also examined by using two-photon imaging. Tissue was prepared as for immunofluorescence. In brief, the uterus was cut into 0.5–1.0 cm length tissue and fixed in 4 % paraformaldehyde, then moved to 30 % sucrose solution overnight. Tissues were removed from the sucrose solution and cut into 100- μ m thick sections after precipitation. The section was moved to the stage of two-photon fluorescence microscope; 920 nm excitation wavelength was chosen. Image was captured at every 1 nm thickness with a 25 \times hydroscope and restructured after 100 shots (FV-1000, Shinjuku, Tokyo, Japan). The results of the imaging were overlapped with the results of H&E staining.

Retrograde tracing of DRG neurons that innervate the uterus

Pirt^{+/+} and *Pirt*^{-/-} mice were anaesthetized with 1 % sodium pentobarbital (40 mg/kg, Merck, Darmstadt, Germany) and restrained in a supine position. A laparotomy was performed via a lower abdomen midline incision, and the uterus was dissected from the bladder. Then, 30 μ L of 1,1'-Diocadecyl-3,3,3',3'-tetramethylindocarbocyanine perchlorate (Dil, 0.25 % in DMSO, Sigma-Aldrich, St. Louis, MO, USA) was gradually instilled into the myometrium and perimetrium through a 50- μ L Hamilton syringe. Different injection sites were chosen randomly in the cervix and body, and each site was swabbed with fresh cotton balls to absorb leaking tracer. After the dye injection, the peritoneal cavity was rinsed with warm saline and the wound was sutured shut. The animals were positioned supine during injection and kept in that position until they recovered from anesthesia. All surgical procedures were performed under sterile conditions. Immunofluorescence and calcium imaging experiments were conducted in mice at 14 days after the dye injection. DRG from spine levels T10–L5 were cut into 10- μ m slices for examination of the retrograde-labeled cells. To calculate the Dil labeled cells in every DRG, every two slices were captured and counted.

Immunostaining of DRG neurons

DRG tissues were collected from spine levels T10–L5, and were then used to immunostain for neurofilament protein-200 (NF-200), plant isolectin B₄ (IB₄), and TRPV1. For immunostaining, we incubated sections in blocking solution (containing 3 % fetal bovine serum, 0.1 % Triton X-100, and 0.02 % sodium azide in PBS) for 2 h at room temperature and then at 4 °C overnight with mouse anti-NF-200 (1:1000; Invitrogen, Grand Island, NY, USA) and isolectin IB₄ Alexa Fluor dye conjugate (1:1000; Invitrogen) primary antibodies. Next, the sections were incubated in Alexa Fluor-conjugated goat anti-mouse IgG (1:100, Earthox, Millbrae, CA, USA) secondary antibody at room temperature for 2 h. Dil-labeled sections were also incubated with rabbit anti-TRPV1 (1:1000; Neuromics, Edina, MN, USA) primary antibodies at 4 °C overnight. Then, the sections were incubated in Alexa Fluor-conjugated donkey anti-rabbit IgG (1:100, molecular probes, Eugene, OR, USA) secondary antibody at room temperature for 2 h. By immunostaining DRG neurons, we counted the number of DRG neurons innervating the uterus, and also measured the diameter of stained neurons using Stereo Investigator 10 software. After each stained picture was captured, it was merged into an image. These neurons of Dil-labeled and fluorescently stained from the same slice were analyzed by using Stereo Investigator 10 analysis software.

Cell culture

Fourteen days after the retrograde tracing procedure, the mice were anesthetized with 1 % sodium pentobarbital. The DRG from spine levels T10–L5 were harvested as previously described [10] and immediately transferred to cold DH10 medium (DMEM/F-12, 10 % FBS, 1 % penicillin–streptomycin–glutamine; Invitrogen). DRGs were washed 2–3 times in warm DH10 and then treated with enzyme solution (5 mg/mL dispase and 1 mg/mL collagenase type I in Hanks Balanced Salt Solution without Ca²⁺ and Mg²⁺, Invitrogen) at 37 °C until the cells dissociated [14, 17]. Dissociated cell suspensions were filtered through a 100- μ m cell strainer (BD, Franklin Lakes, NJ, USA). After being centrifuged at 1500 rpm for 5 min, DRG neurons were resuspended in DH10, and nerve growth factor was added (50 ng/mL, Millipore, Billerica, MA, USA). Fifty microliters of suspended cells in solution were plated onto pre-sterilized glass coverslips that had been coated with 0.5 mg/mL poly-D-lysine (Biomedical Technologies, Inc., Stoughton, MA, USA) and 10 μ g/mL laminin (Invitrogen). Plated neurons were cultured in an incubator (95 % O₂ and 5 % CO₂) at 37 °C and used for calcium imaging studies within 48 h.

Calcium imaging

The DRG neurons were loaded with fura-2-acetomethoxy ester (Molecular Probes, Eugene, OR, USA) for 30 min at 37 °C in the dark in accord with previous studies [14, 17]. After being washed 3 times with PBS, the glass coverslips were placed into a chamber and perfused with a solution containing 137 mM NaCl, 5.4 mM KCl, 1.2 mM MgCl₂, 1.2 mM NaH₂PO₄, 1 mM CaCl₂, 10 mM glucose, and 20 mM HEPES (pH 7.4). A high-speed continuously scanning monochromatic light source (Polychrome V, Till Photonics, Gräfeling, Germany) was used for excitation at 340 and 380 nm, enabling us to detect changes in intracellular free calcium concentration.

Data analysis

The methods for statistical comparison in each study are given in the Results section. The number of animals used in each study was based on our experiences and on similar studies. We grouped seven pairs of female *Pirt*^{+/+} and *Pirt*^{-/-} littermates for use in the experimental group and the control group in the behavioral experiments. The genotype of mice was blinded to experimenters to reduce selection and observation bias. After the experiments were completed, no data point was excluded. Paired sample *t* tests (Spass 16.0) were used to compare the behavioral results. For morphological results, we used representative data from three mice with similar results. Statistical analysis of the number of Dil-labeled cells, *Pirt*-positive cells, and IB₄-binding cells were carried out manually. We used representative data from Ca²⁺ imaging studies that were replicated at least 15 times from 3 mice (5 times in each mouse). We used independent sample *t* tests (Spass 16.0) to calculate the proportion of cells that responded and the intensity of response. *P* < 0.05 was considered statistically significant in all tests.

Results

Pirt^{-/-} mice exhibit less UCP than *Pirt*^{+/+} mice

To investigate the role of *Pirt* in UCP, we first examined writhing behavior induced by intraperitoneal injection of oxytocin in *Pirt*^{+/+} and *Pirt*^{-/-} female mice after 6 days of priming with estradiol benzoate (*n* = 7/group). UCP in mice can be inferred by the stretching of the posterior limb followed by an abdominal contraction [16, 18, 19]. The number of writhing responses during the 80 min after oxytocin injection was significantly less in *Pirt*^{-/-} mice (3.1 ± 0.7) than in *Pirt*^{+/+} mice (8.4 ± 1.6, *P* < 0.01, paired *t* test Spass 16.0; Fig. 1b). The writhing responses often occurred in two phases (1st phase: 0–30 min; 2nd phase: 40–60 min after oxytocin injection, Fig. 1a), and subsided after 80 min. The decreased number of writhing responses in *Pirt*^{-/-} mice suggests an involvement of

Pirt in UCP. The expression levels of *Pirt* were detected in UCP and normal mice DRG neurons by real-time PCR. We found no changes of *Pirt*-expressing in UCP (*p* > 0.05, *n* = 4, Fig. 1c).

Pirt-expressing nerve fibers innervate the uterus

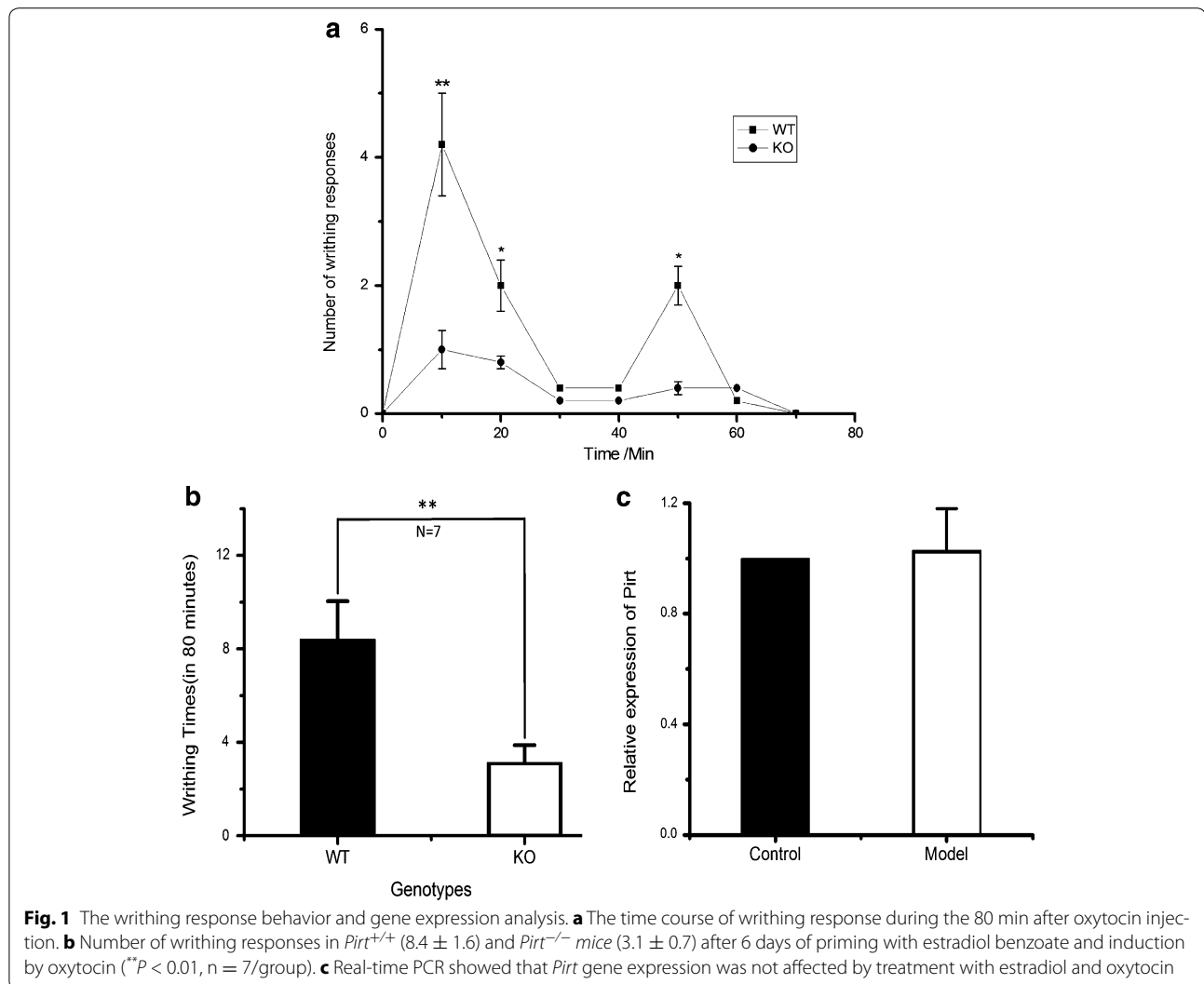
Pirt is specifically expressed in DRG neurons in the peripheral nervous system [14]. As shown above, *Pirt*^{-/-} mice exhibited a less intensive writhing response than that of *Pirt*^{+/+} mice (Fig. 1), which led us to speculate that *Pirt*-expressing nerve fibers may innervate the uterus. In *Pirt*^{-/-} mice, the *Pirt*-coding region was replaced with a green fluorescent protein (GFP)-expressing construct (Fig. 2a–f). Thus, *Pirt*-expressing DRG neurons and their branches can be visualized by GFP fluorescence. By superimposing the bright-field H&E-staining over the fluorescence image of the same section, we found *Pirt*-expressing nerve fibers distribution in the myometrium of uterus (Fig. 2d–f). Subsequent two-photon microscopy imaging confirmed this finding (Fig. 2g–h).

DRG neurons innervating the uterus are *Pirt*-positive

Next, we further characterized the neurochemical properties of DRG neurons projecting to the uterus using retrograde labeling. Fourteen days after injection of Dil into the uterus, DRGs from thoracic and lumbar levels were isolated and examined given that hypogastric nerves innervating the uterine cervix and uterus originate primarily from T12–L2 DRGs [1, 10, 20]. We differentiated Dil-traced fibers from untraced fibers by overlapping Dil-labeling with bright-field images (Fig. 3c). The number of Dil-labeled DRG neurons at each level was as follows: T10, 148 ± 23; T11, 213 ± 21; T12, 358 ± 40; T13, 533 ± 46; L1, 263 ± 35; L2, 330 ± 28; L3, 127 ± 17; L4, 102 ± 14; and L5, 98 ± 16 (*n* = 3). Because the number of Dil-labeled cells was highest at T13, we thus further measured the size of Dil-labeled DRG neurons at this level. Most Dil-labeled DRG neurons were small-to-medium size with a surface area ranging from 100 to 600 μm² (Fig. 3d). Immunostaining revealed that Dil-labeled neurons were not overlapped with NF200 stained neurons (Fig. 4a–c); 96.4 % of Dil-labeled DRG neurons were IB₄-binding neurons (Fig. 4d–f) and 96 % of Dil-labeled DRG neurons were *Pirt*-positive (Fig. 4g–i). By double staining, 25 % of *Pirt*-expressing cells were TRPV1 positive, 46 % of *Pirt*-expressing cells were Dil-labeled, 31 % of Dil-labeled cells were TRPV1 positive (Fig. 4j–m).

The percentage of capsaicin-response DRG neurons is more in *Pirt*^{+/+} mice than in *Pirt*^{-/-} mice

To further investigate the involvement of *Pirt* in UCP, we conducted a Ca²⁺ imaging study to compare the



capsaicin-evoked response of Dil-labeled DRG neurons from *Pirt*^{+/+} and *Pirt*^{-/-} mice (Fig. 5a–d). The proportion of Dil-labeled DRG neurons responding to capsaicin in *Pirt*^{+/+} mice was significantly higher (31.4 ± 4.4 %) than the proportion in *Pirt*^{-/-} mice (17.8 ± 3.0 %, *P* < 0.05, *n* = 3 animals/group, Fig. 5e). In *Pirt*^{+/+} mice, 46 % (382 of 816) of Pirt-positive cells were Dil-labeled cells, in which 31 % (120 of 382) responded to capsaicin (Fig. 5f). By contrast, in *Pirt*^{-/-} mice, only 25 % (204 of 816) of Dil-labeled neurons responded to capsaicin.

Discussion

Pirt is a phosphoinositide-binding protein that functions as a key regulatory subunit of the TRPV1 channel, which may be involved in visceral pain [14]. In the present study, we investigated the role of Pirt in the perception of UCP in female mice. We found that—after a 6-day period

of estradiol priming and an oxytocin challenge—*Pirt*^{-/-} mice exhibited markedly reduced writhing behavior than their *Pirt*^{+/+} counterparts. In uterus, Pirt-expressing nerve terminals were limited to the myometrium. Importantly, Pirt-expressing DRG neurons innervating the uterus could respond to capsaicin. Furthermore, the proportion of DRG neurons responding to capsaicin was reduced in *Pirt*^{-/-} mice compared to that in *Pirt*^{+/+} mice. Altogether, our findings suggest that Pirt contributes to UCP.

Sex hormones play an important role in visceral pain hypersensitivity [21, 22]. In animal models of uterine contraction, estrogen-induced hyperalgesia was associated with increased TRPV1 expression in primary sensory neurons innervating the uterus [10], which showed that afferent responses to cervical distension were reduced by the antagonist of capsaicin (capsazepine)

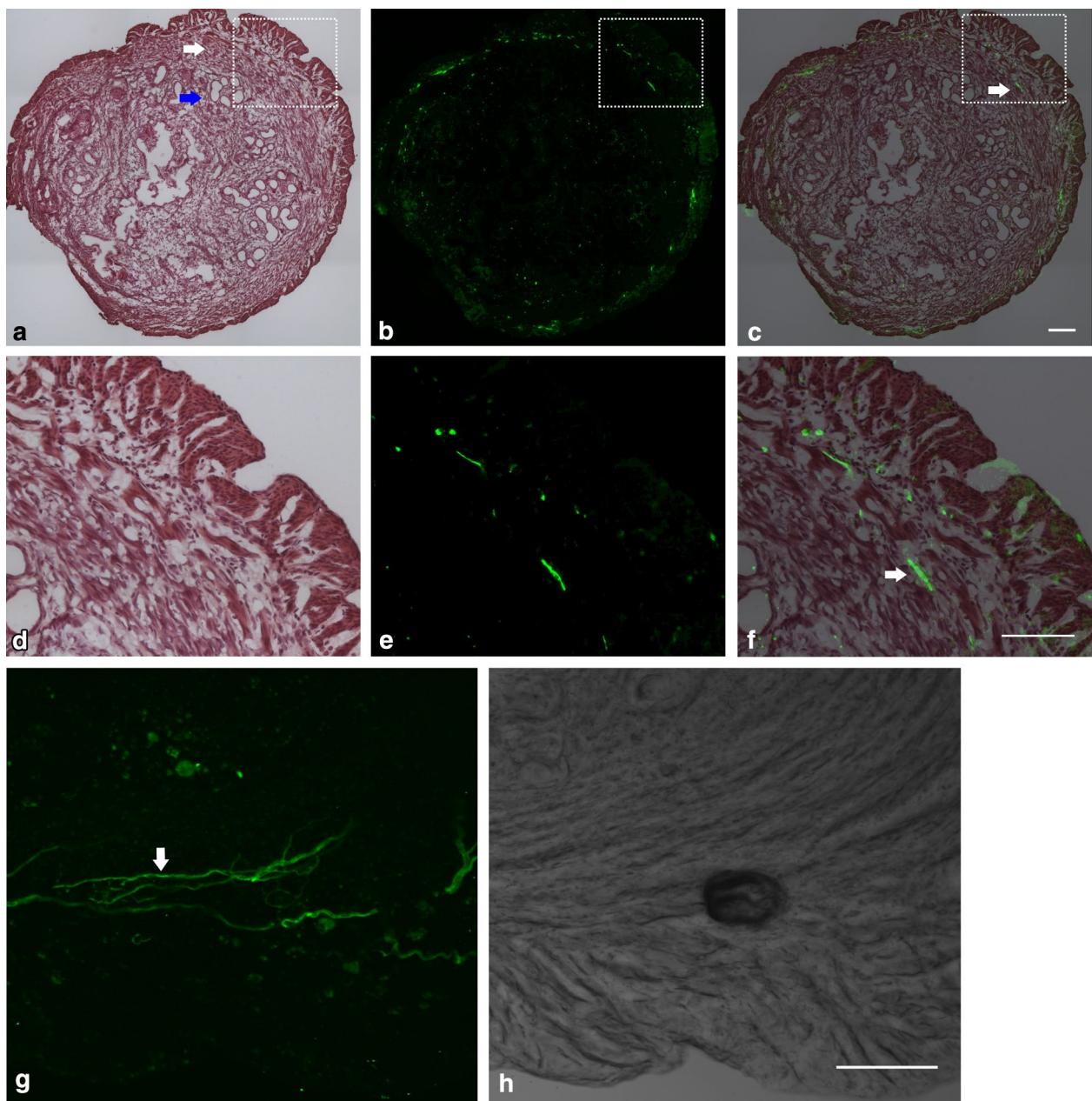
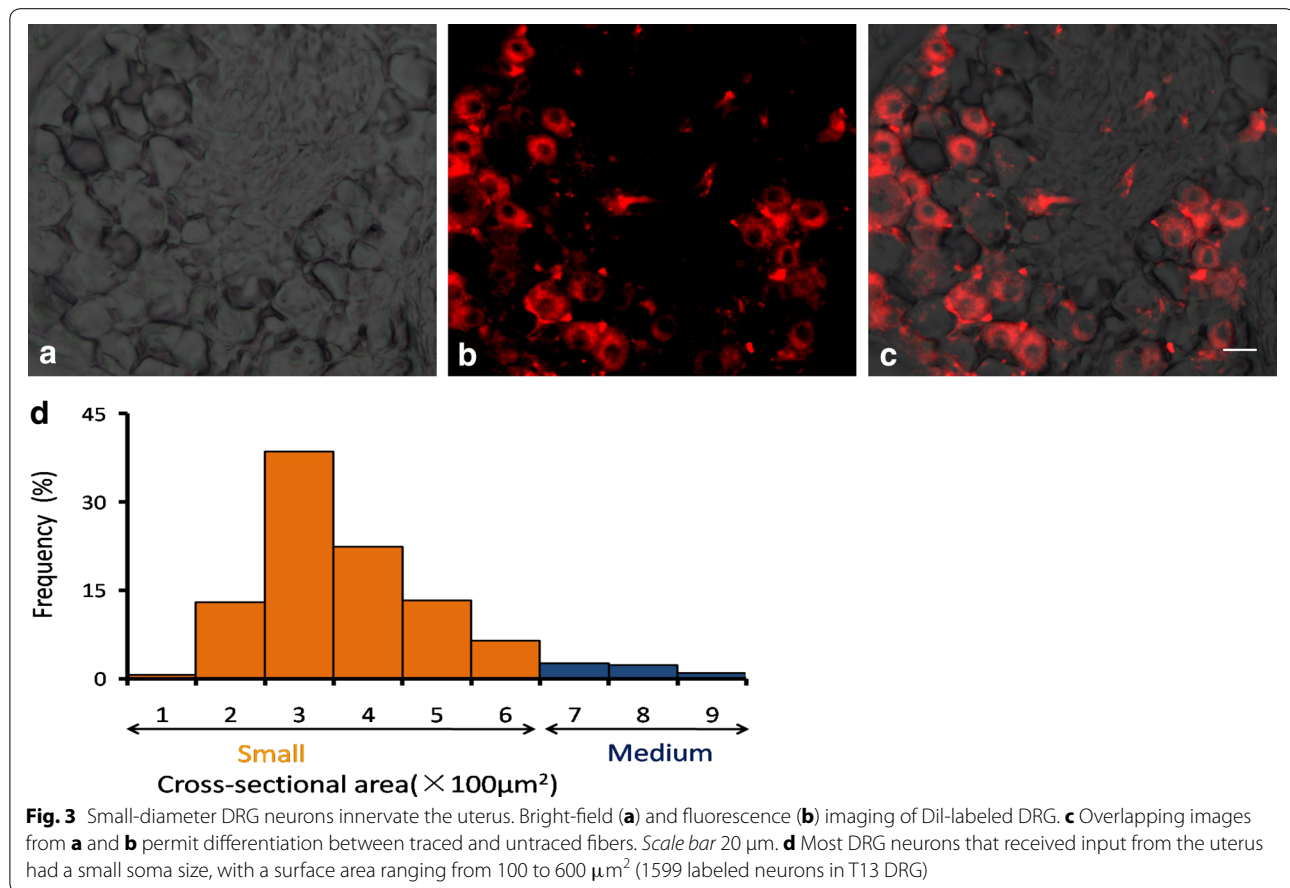


Fig. 2 Pirt-expressing nerves innervate the uterus. **a** Hematoxylin and eosin-stained section of the uterus. Myometrium and endometrium are indicated by *white arrow* and *blue arrow*, respectively. **b** Image of the uterine section under fluorescence microscopy. In *Pirt*^{-/-} mice, the entire Pirt-coding region was replaced by an EGFP-IRESrtTA-ACN-targeting construct, which expresses green fluorescent protein. Thus, Pirt-expressing fibers can be identified by *green fluorescence*. **c** Superimposed images of **a** and **b**. Pirt-expressing fiber is indicated by a *white arrow*. **d-f** Higher resolution views of the *boxed areas* in **a-c**, respectively. Fluorescence (**g**) and bright-field (**h**) images from two-photon microscopy analysis showing Pirt-expressing nerve fibers in the myometrium (*white arrow*). Scale bar 100 μ m

in estrogen-treated animals [11]. However, estrogen did not affect the expression of Pirt. Based on these findings, we administered the estrogen to female mice for 6 days

to prime the induction of pain hypersensitivity to uterine contractions; then, we administered the oxytocin on day 7 to evoke an UCP, as shown previously [18, 19].

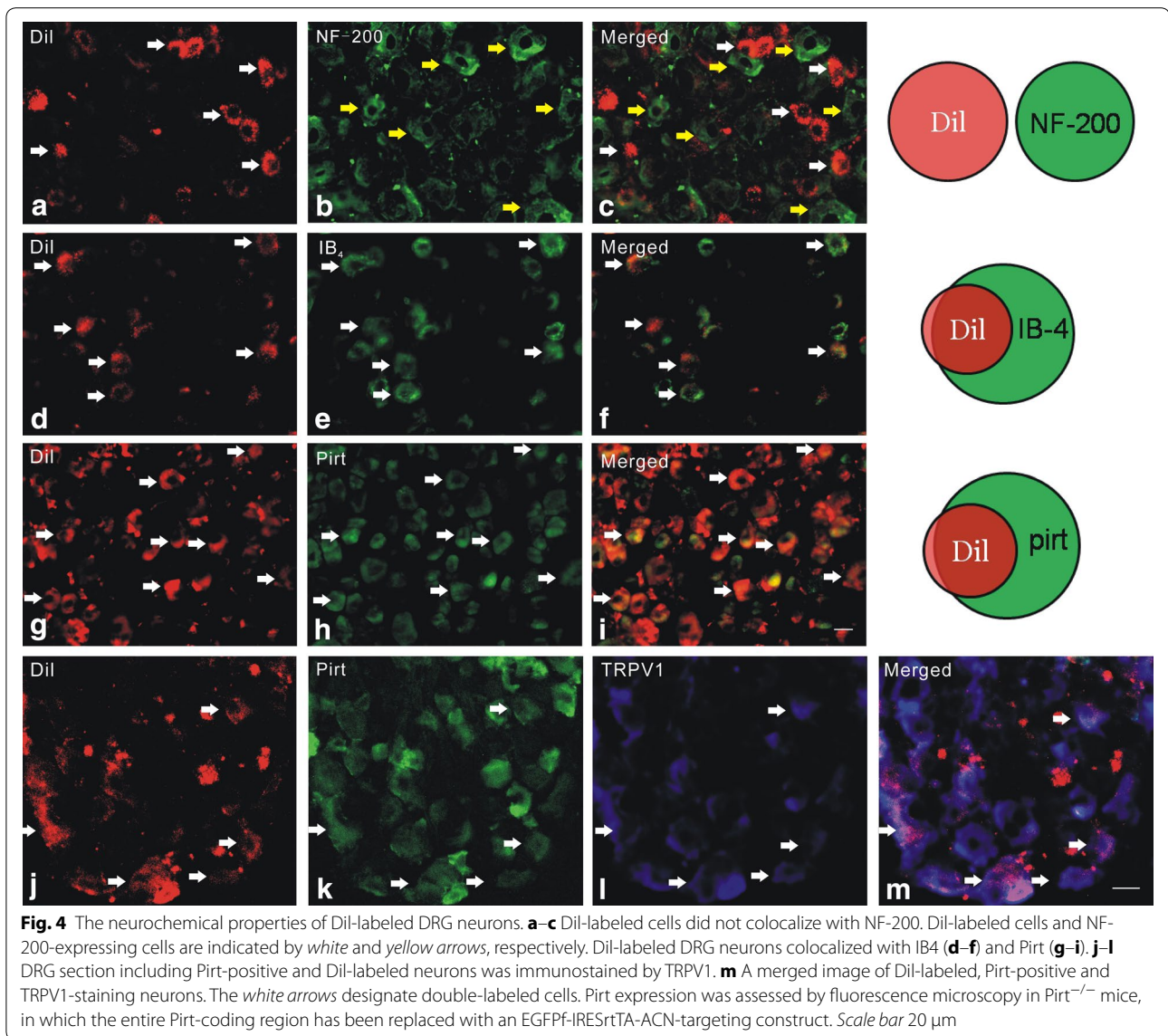


Writhing behavior—which may indicate the presence of visceral pain—was less evident in *Pirt*^{-/-} mice than in *Pirt*^{+/+} mice. These observations suggest an involvement of *Pirt* in UCP. Interestingly, the writhing response was manifested in two phases after oxytocin injection, similar to that of formaldehyde-induced inflammatory pain [23, 24]. Although the mechanisms remain unclear, we postulate that the first phase may result from a direct action of oxytocin on the uterus, while the second phase may involve a sensitization of dorsal horn neurons and the release of algogenic factors after uterine contraction.

Pirt is expressed in most nociceptive DRG neurons, including TRPV1-positive cells. Previously, it was reported that *Pirt*^{-/-} mice show an impaired pain response to noxious heat stimuli and capsaicin [14]. Interestingly, *Pirt*^{-/-} mice also exhibited decreased responses to cold stimuli, suggesting that *Pirt* may also regulate cold-receptor TRPM8 function [15]. The pain originating from labor and gynecological disorders results primarily from distension of the uterine cervix and lower uterine segment [2, 10, 11]. We show here for the first time that *Pirt*-expressing nerve terminals innervate

the myometrium of the uterus, providing a physiological basis for its involvement in UCP. There have been indications in the literature that female reproductive tract tissues (cervix and caudal uterus), as well as other abdominal organs such as the bladder and distal colon, are innervated by DRG neurons in T10–L2 segments [10, 25]. Visceral pain from pancreas, bladder, and colon has been proposed to be mediated by non-peptidergic, small-diameter DRG neurons [25, 26]. Our current findings support this point of view. Additionally, we show for the first time that DRG neurons that innervate the uterus are entirely *Pirt*-positive. Therefore, our studies support the concept that *Pirt*-expressing DRG neurons constitute a critical component of the pain transduction pathway involved in UCP.

TRPV1 can be activated by noxious heat stimuli and capsaicin [27]. Investigators have also recently analyzed the general architecture and physiological function of TRP-type channels [28, 29]. TRPV1-positive nerve fibers were found in the uterus, and TRPV1 was shown to be involved in UCP. For example, TRPV1 was suggested to play an important role



in estrogen-induced sensitization of cervical afferents [10, 11]. Activation of TRPV1 receptors in nerve fibers that innervate the uterus also induced sensitization of the pelvic-urethra reflex [12]. Mechanical stimulation of somatosensory neurons induced physical interactions between the C-terminus of TRPV1 and microtubules of the cell [30], suggesting that TRPV1 has a role in transduction of mechanical stimuli. Pirt can bind

to TRPV1 and positively regulate its function [14]. In our study, uterine DRG neurons from *Pirt*^{+/+} mice showed a higher response rate to capsaicin challenge than those from *Pirt*^{-/-} mice. As the binding of Pirt increased the excitability of TRPV1-expressing neurons [14], we reason that Pirt may play an important role in UCP through its interaction with TRPV1.

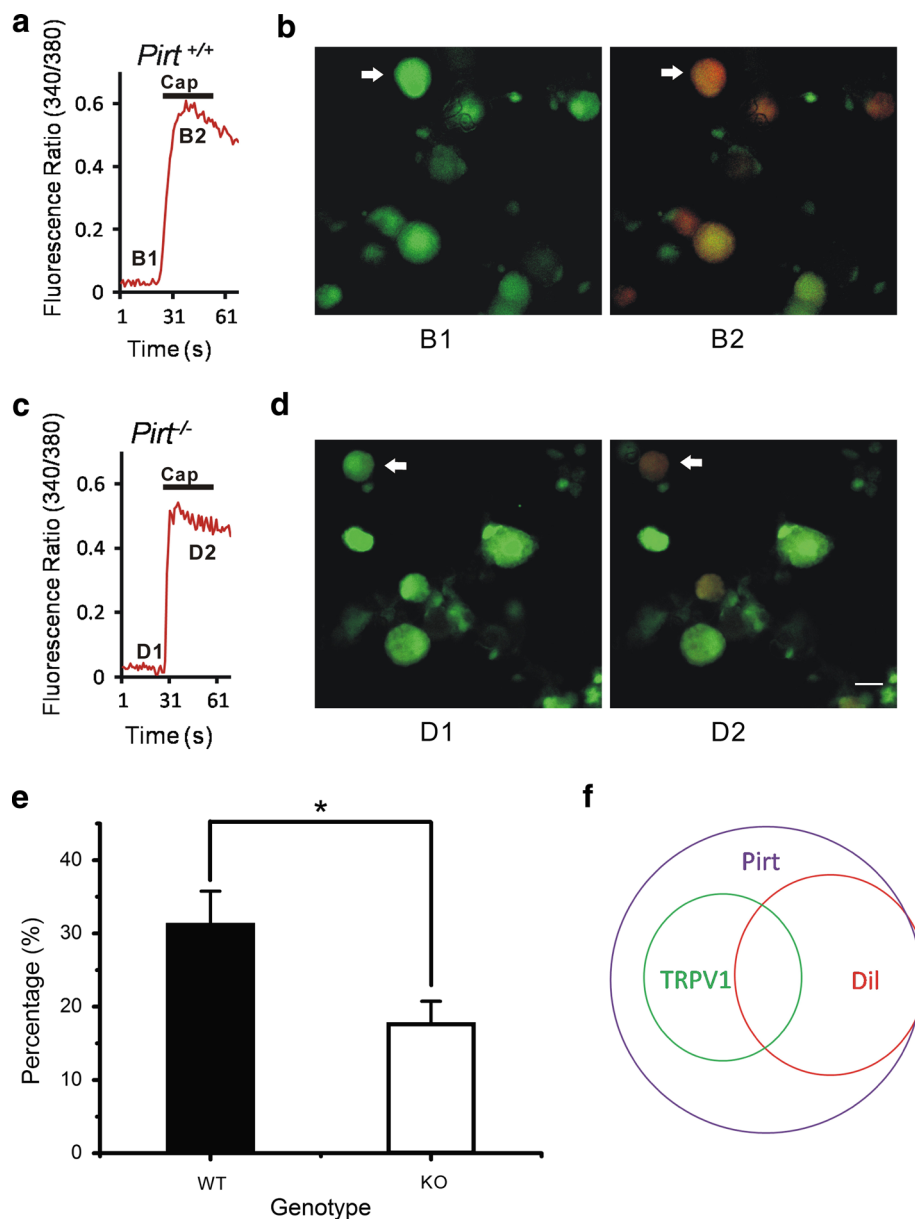


Fig. 5 Dil-labeled DRG neurons respond to capsaicin. **a** Representative capsaicin-induced Ca^{2+} trace in DRG neuron from *Pirt*^{+/+} mouse. **b** Images of DRG neurons from *Pirt*^{+/+} mice before (B1) and after (B2) capsaicin treatment (5 μM). **c** Representative capsaicin-induced Ca^{2+} trace in DRG neuron from *Pirt*^{+/+} mouse. **d** Images of DRG neurons from *Pirt*^{-/-} mice before (D1) and after (D2) capsaicin. Scale bar 20 μm . **e** The proportion of DRG neurons from *Pirt*^{+/+} and *Pirt*^{-/-} mice that responded to capsaicin (% of total cells, * $P < 0.05$, $n = 3/\text{group}$). **f** 382 of 816 accounted *Pirt*^{+/+} positive cells were Dil-labeled cells (46 %). 120 of 382 Dil-labeled cells (31 %) responded to capsaicin. 204 of 816 *Pirt*^{+/+} neurons (25 %) responded to capsaicin

Conclusion

Our findings indicate that *Pirt* plays a significant role in uterine contraction-induced pain (UCP) by comparison of behavior tests in *Pirt*^{-/-} mice and *Pirt*^{+/+} mice, the analysis of immunohistochemistry and calcium imaging on DRG neurons.

Abbreviations

Pirt: phosphoinositide interacting regulator of transient receptor potential; UCP: uterine contraction-induced pain; TRPV1: transient receptor potential vanilloid channel 1; DRG: dorsal root ganglia; CNS: central nervous system; NF-200: neurofilament protein-200; IB₄: plant lectin B₄; Dil: 1,1'-Diocadecyl-3,3',3'-tetramethylindocarbocyanine perchlorate; OCT: optimum cutting temperature compound.

Authors' contributions

CW collected and analyzed the data and drafted the manuscript; YY helped with the retrograde labeling; ZW performed the two-photon confocal imaging; CZ performed animal breeding; GW, GY, NY, HS, MT, and QH helped breed the animals, participated in animal models and genotyping experiments. LL, QL, YG, and XD were involved in the discussion of data and writing of this manuscript. JD helped with the experimental design. ZT designed the whole experiment and wrote the final manuscript. All authors read and approved the final manuscript.

Author details

¹ College of Basic Medicine, Nanjing University of Chinese Medicine, 138 Xianlin Rd, Nanjing 210023, Jiangsu, China. ² College of Life Science, Nanjing Normal University, Nanjing 210046, Jiangsu, China. ³ Department of Anesthesiology, University of Washington, St. Louis, MO 63110, USA. ⁴ Department of Anesthesiology and Critical Care Medicine, School of Medicine, Johns Hopkins University, Baltimore, MD 21205, USA. ⁵ The Solomon H. Snyder Department of Neuroscience, Center for Sensory Biology, School of Medicine, Johns Hopkins University, Baltimore, MD 21205, USA.

Acknowledgements

This work was supported by the Chinese Natural Science Foundation to Z-XT (31271181, 31471007), by the Overseas and Hong Kong, Macau Scholars Collaborative Research Fund to X-ZD (31328012), from the Project Funded by the Priority Academic Program Development of Jiangsu Higher Education Institutions (PAPD), sponsored by the "Qing Lan Project" in Jiangsu Province, and from the Jiangsu Collaborative Innovation Center of Traditional Chinese Medicine (TCM) Prevention and Treatment of Tumor.

Compliance with ethical guidelines**Competing interests**

The authors declare that they have no competing interests.

Received: 5 May 2015 Accepted: 21 August 2015

Published online: 17 September 2015

References

- Berkley KJ, Hotta H, Robbins A, Sato Y. Functional properties of afferent fibers supplying reproductive and other pelvic organs in pelvic nerve of female rat. *J Neurophysiol*. 1990;63:256–72.
- Liu B, Eisenach JC, Tong C. Chronic estrogen sensitizes a subset of mechanosensitive afferents innervating the uterine cervix. *J Neurophysiol*. 2005;93:2167–73.
- Birder LA, Nakamura Y, Kiss S, Nealen ML, Barrick S, Kanai AJ, Wang E, Ruiz G, De Groat WC, Apodaca G, Watkins S, Caterina MJ. Altered urinary bladder function in mice lacking the vanilloid receptor TRPV1. *Nat Neurosci*. 2002;5:856–60.
- Jones RC III, Xu L, Gebhart GF. The mechanosensitivity of mouse colon afferent fibers and their sensitization by inflammatory mediators require transient receptor potential vanilloid 1 and acid-sensing ion channel 3. *J Neurosci*. 2005;25:10981–9.
- Rong W, Hillsley K, Davis JB, Hicks G, Winchester WJ, Grundy D. Jejunal afferent nerve sensitivity in wild-type and TRPV1 knockout mice. *J Physiol*. 2004;560:867–81.
- Winston JH, Sarna SK. Developmental origins of functional dyspepsia-like gastric hypersensitivity in rats. *Gastroenterology*. 2013;144:570–9.
- Craft RM, Mogil JS, Aloisi AM. Sex differences in pain and analgesia: the role of gonadal hormones. *Eur J Pain*. 2004;8:397–411.
- Li LH, Wang ZC, Yu J, Zhang YQ. Ovariectomy results in variable changes in nociception, mood and depression in adult female rats. *PLoS One*. 2014;9:e94312.
- Rowan MP, Berg KA, Roberts JL, Hargreaves KM, Clarke WP. Activation of estrogen receptor alpha enhances bradykinin signaling in peripheral sensory neurons of female rats. *J Pharmacol Exp Ther*. 2014;349:526–32.
- Tong C, Conklin D, Clyne BB, Stanislaus JD, Eisenach JC. Uterine cervical afferents in thoracolumbar dorsal root ganglia express transient receptor potential vanilloid type 1 channel and calcitonin gene-related peptide, but not P2X3 receptor and somatostatin. *Anesthesiology*. 2006;104:651–7.
- Yan T, Liu B, Du D, Eisenach JC, Tong C. Estrogen amplifies pain responses to uterine cervical distension in rats by altering transient receptor potential-1 function. *Anesth Analg*. 2007;104:1246–50 (**tables**).
- Peng HY, Chang HM, Lee SD, Huang PC, Chen GD, Lai CH, Lai CY, Chiu CH, Tung KC, Lin TB. TRPV1 mediates the uterine capsaicin-induced NMDA NR2B-dependent cross-organ reflex sensitization in anesthetized rats. *Am J Physiol Renal Physiol*. 2008;295:F1324–35.
- Nie J, Liu X, Guo SW. Immunoreactivity of oxytocin receptor and transient receptor potential vanilloid type 1 and its correlation with dysmenorrhea in adenomyosis. *Am J Obstet Gynecol*. 2010;202:346–8.
- Kim AY, Tang Z, Liu Q, Patel KN, Maag D, Geng Y, Dong X. Pirt, a phosphoinositide-binding protein, functions as a regulatory subunit of TRPV1. *Cell*. 2008;133:475–85.
- Tang Z, Kim A, Masuch T, Park K, Weng H, Wetzel C, Dong X. Pirt functions as an endogenous regulator of TRPM8. *Nat Commun*. 2013;4:2179.
- Reichert JA, Daughters RS, Rivard R, Simone DA. Peripheral and preemptive opioid antinociception in a mouse visceral pain model. *Pain*. 2001;89(2–3):221–7.
- Liu Q, Tang Z, Surdenikova L, Kim S, Patel KN, Kim A, Ru F, Guan Y, Weng HJ, Geng Y, Udem BJ, Kollarik M, Chen ZF, Anderson DJ, Dong X. Sensory neuron-specific GPCR Mrgprs are itch receptors mediating chloroquine-induced pruritus. *Cell*. 2009;139:1353–65.
- Liu P, Duan JA, Hua YQ, Tang YP, Yao X, Su SL. Effects of xiang-fu-si-wu decoction and its main components for dysmenorrhea on uterus contraction. *J Ethnopharmacol*. 2011;133:591–7.
- Sun HY, Cao YX, Liu J, Gao JW, Ma M. The establishment of the dysmenorrhea model in mice. *Chin Pharmacol Bull*. 2002;18:233–5.
- Berkley KJ, Robbins A, Sato Y. Afferent fibers supplying the uterus in the rat. *J Neurophysiol*. 1988;59:142–63.
- Mogil JS. Sex differences in pain and pain inhibition: multiple explanations of a controversial phenomenon. *Nat Rev Neurosci*. 2012;13:859–66.
- Sanoja R, Cervero F. Estrogen-dependent abdominal hyperalgesia induced by ovariectomy in adult mice: a model of functional abdominal pain. *Pain*. 2005;118:243–53.
- Berta T, Park CK, Xu ZZ, Xie RG, Liu T, Lu N, Liu YC, Ji RR. Extracellular caspase-6 drives murine inflammatory pain via microglial TNF-alpha secretion. *J Clin Invest*. 2014;124:1173–86.
- Fischer M, Carli G, Raboisson P, Reeh P. The interphase of the formalin test. *Pain*. 2014;155:511–21.
- Christianson JA, Liang R, Ustinova EE, Davis BM, Fraser MO, Pezzone MA. Convergence of bladder and colon sensory innervation occurs at the primary afferent level. *Pain*. 2007;128:235–43.
- Fasanella KE, Christianson JA, Chanthaphavong RS, Davis BM. Distribution and neurochemical identification of pancreatic afferents in the mouse. *J Comp Neurol*. 2008;509:42–52.
- Caterina MJ, Schumacher MA, Tominaga M, Rosen TA, Levine JD, Julius D. The capsaicin receptor: a heat-activated ion channel in the pain pathway. *Nature*. 1997;389:816–24.
- Cao E, Liao M, Cheng Y, Julius D. TRPV1 structures in distinct conformations reveal activation mechanisms. *Nature*. 2013;504:113–8.
- Liao M, Cao E, Julius D, Cheng Y. Structure of the TRPV1 ion channel determined by electron cryo-microscopy. *Nature*. 2013;504:107–12.
- Prager-Khoutorsky M, Khoutorsky A, Bourque CW. Unique interweaved microtubule scaffold mediates osmosensory transduction via physical interaction with TRPV1. *Neuron*. 2014;83:866–78.